https://doi.org/10.5194/egusphere-2023-1851
Preprint. Discussion started: 4 September 2023

Response of $PM_{2.5}$ chemical composition to variations in anthropogenic emissions and meteorological conditions during COVID-19 lockdown

Yitian Gong[1], Haijun Zhou[1,2,3*], Xi Chun[1,2,3], Zhiqiang Wan[1,2,3], Jingwen Wang[1], Chun Liu[1]

[1]College of Geographical Sciences, Inner Mongolia Normal University, Hohhot 010022, China
[2]Provincial Key Laboratory of Mongolian Plateau's Climate System, Inner Mongolia Normal University, Hohhot 010022, China
[3]Inner Mongolia Repair Engineering Laboratory of Wetland Eco-environment System, Inner Mongolia Normal University, Hohhot 010022, China

Correspondence to: Haijun Zhou (hjzhou@imnu.edu.cn)

Abstract: $PM_{2.5}$ is a primary atmospheric pollutant with various sources and complicated chemical compositions that are influenced by various factors, such as anthropogenic emissions (AE) and meteorological conditions (MC). MC have significant impacts on variations of the atmospheric pollutant; therefore, emission reduction policies and ambient air quality are non-linearly correlated, which hinders accurate assessments of the effectiveness of control measures. The online observations of $PM_{2.5}$ and its chemical composition were conducted in Hohhot, China, from December 1, 2019, to February 29, 2020, to investigate $PM_{2.5}$ chemical compositions respond to the variation of AE and MC. Moreover, the random forest (RF) model was used to quantify the AE and MC contributions of $PM_{2.5}$ and its chemical composition during severe hazes and the COVID-19 pandemic lockdown period. During the clean period, MC contributed -124% to $PM_{2.5}$ concentrations, indicating that MC promoted $PM_{2.5}$ dispersion. During severe pollution episodes, MC contributed 49% to $PM_{2.5}$ concentrations, indicating that MC promoted $PM_{2.5}$ accumulation. The inorganic aerosols (SO_4^{2-}, NO_3^-, and NH_4^+) showed the strongest response to MC. MC had significant contributions to the $PM_{2.5}$ (36%), SO_4^{2-} (32%), NO_3^- (29%), NH_4^+ (28%), OC (22%), and SOC (17%). From the pre-lockdown to lockdown period, AE (MC) contributed 52% (48%), 81% (19%), 48% (52%), 68% (32%), 59% (41%), and 288% (-188%) to the $PM_{2.5}$, SO_4^{2-}, NO_3^-, NH_4^+, OC, and SOC

https://doi.org/10.5194/egusphere-2023-1851
Preprint. Discussion started: 4 September 2023

variations, respectively. The variations of MC (especially the increase in relative humidity) rapidly generated meteorologically sensitive species (SO_4^{2-}, NO_3^-, and NH_4^+), which led to severe winter pollution. This study provides reference for assessing the net benefits of emission reduction measures for $PM_{2.5}$ and its chemical compositions.

1 Introduction

Due to the increasing levels of industrialization and urbanization, air pollution in China has attracted a significant concern (Fuzzi et al., 2015). Frequent pollution episodes primarily driven by $PM_{2.5}$ have emerged as a crucial environmental challenge (Zhang et al., 2012). To improve the ambient air quality, China has implemented many strict strategies, resulting in a substantial decline in $PM_{2.5}$ (Zhang and Zheng, 2019). However, it remains a challenge to meet the new guideline of WHO (WHO, 2021). Particularly in northern China, the frequency of severe episodes remains high (An et al., 2019). The chemical composition of $PM_{2.5}$ is very complex, which is influenced by anthropogenic emissions (AE) and meteorological conditions (MC). The rapid generation of secondary inorganic aerosols (sulfates, nitrates, and ammonium, SNA) under adverse MC is the driving factor of severe haze in China (Yang et al., 2011).

In December 2019, the coronavirus pandemic (COVID-19) outbreak occurred in China. To prevent the spread of the virus, China implemented various control measures, including transport restrictions and home quarantine (Yang et al., 2022a). Due to reduced socio-economic activities during the lockdown period (LD), NOx emissions across China decreased by 36% (Feng et al., 2020). However, despite a substantial reduction in primary emissions during LD, unexpected hazes occurred in Northern China Plan (Wang et al., 2020) and the Yangtze River Delta (YRD) region (Huang et al., 2021). It can be attributed to the counteracting effect of secondary aerosols induced by adverse MC. The variation of MC contributed over 70% of the $PM_{2.5}$ variations in China (He et al., 2017). MC are essential factors driving the

https://doi.org/10.5194/egusphere-2023-1851
Preprint. Discussion started: 4 September 2023

variations of atmospheric pollutants (Dominici et al., 2002). Therefore, quantifying the impacts of AE and MC on atmospheric pollutants is crucial for understanding haze events. Lockdown measures provided a opportunity to estimate the response of $PM_{2.5}$ chemical composition to the variations of AE and MC; thus, evaluations of this period can shed light on the intricate non-linear correlation between air quality and emission reduction policies.

Random forest (RF) model demonstrated sound performance in predicting environmental air quality and quantifying MC contributions (Grange et al., 2018). Furthermore, it can elucidate the relationship between independent predictors and dependent variables and reveal the importance of influencing factors (Vu et al., 2019). Zhang (Zhang et al., 2023) applied RF model to quantify the impacts of AE and MC on $PM_{2.5}$ variations in Tibetan Plateau. The result suggested that the reduction in AE was the main driver for reducing $PM_{2.5}$ in the region. Chen (Chen et al., 2023)found that from 2015 to 2019, the contributions of AE (MC) to the $PM_{2.5}$ in Henan Province, Beijing-Tianjin-Hebei, and the YRD region were -41.8 (27.0), -38.6 (12.3), and -31.3 (2.9) $\mu g/m^3$, respectively. Liu (2022) observed that in Hubei province during LD, the changes in AE reduced $PM_{2.5}$ by 33.3%, whereas variations in MC increased $PM_{2.5}$ contents by 8.8% compared to 2019. The adverse MC resulted in a 9.8% increase in $PM_{2.5}$ in North China during LD, whereas the reduction in AE induced a 32.2% decrease in $PM_{2.5}$ concentrations (Lv et al., 2023). In conclusion, significant differences have been observed in the response of $PM_{2.5}$ concentrations to AE reductions and variations in MC in different regions. The contribution of MC to $PM_{2.5}$ chemical composition remains poorly understood.

The present study employed online observations of $PM_{2.5}$ chemical composition in Hohhot to reveal the response of $PM_{2.5}$ chemical compositions to AE and MC. The RF model was utilized to quantify the contributions of AE and MC to $PM_{2.5}$ chemical composition during severe pollution episodes and LD, revealing the intricate non-linear correlations between the chemical composition of $PM_{2.5}$ and AE and MC.

https://doi.org/10.5194/egusphere-2023-1851
Preprint. Discussion started: 4 September 2023

2 Data and Methods

2.1 Data Sources

Eight water-soluble ions (SO_4^{2-}, NO_3^-, NH_4^+, Cl^-, K^+, Ca^{2+}, Na^+, and Mg^{2+}) were observed using an online ion chromatograph (MARGA, Metrohm, Switzerland) at Environmental Monitoring Center of Inner Mongolia (Fig. 1). The hourly concentrations of organic carbon (OC) and elemental carbon (EC) were measured using an online OC/EC analyzer (Model 4, Sunset Lab, USA). The concentrations of metals (K, Ca, Fe, Zn, Cu, Ba, Pb, Mn, Ti, Cr, V, Sc, Sn, Ni, Cs, Br, Sb, Se, Co, As, Ag, Tl, Mo, Cd, Cs, and Te) were obtained using an online atmospheric metal monitoring system (AMMS-100, Focused Photonics Inc., China). The hourly concentrations of atmospheric pollutants and meteorological variables were simultaneously measured at the same site.

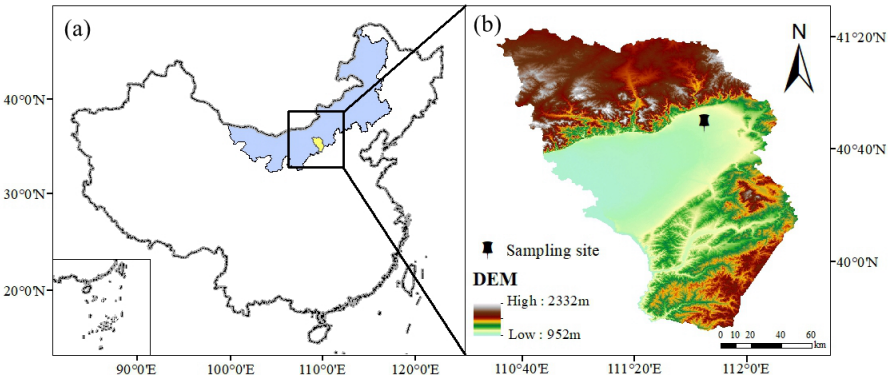

Figure 1. Location of the (a) study area and (b) sampling sate

2.2 RF Model

RF model was used to quantify the contribution of AE and MC to atmospheric pollutants (Grange et al., 2018). The hourly data (70% for training, 30% for testing) of pollutant concentrations, meteorological parameters, and time variables were input into the model to predict the pollutant concentrations free from the influence of MC. The difference between observed and predicted values represents the MC contribution

https://doi.org/10.5194/egusphere-2023-1851
Preprint. Discussion started: 4 September 2023

to atmospheric pollutant concentrations (Guo et al., 2022). We assessed the model performance using nine statistical indicators (Table S1). The results indicated that all the performance metrics for pollutant predictions met the required criteria, indicating that the model possesses adequate predictive capability and performance.

3 Results and discussion

3.1 Variations in pollutant concentrations

The time series of meteorological variables and atmospheric pollutants in Hohhot are presented in Fig. 2. Thirty-three daily $PM_{2.5}$ concentrations exceeded the National Ambient Air Quality Standard (75 $\mu g \cdot m^{-3}$), which accounted for 36.2% of the total sampling days. Seven pollution episodes ($PM_{2.5}$ daily concentrations exceeding 75 $\mu g \cdot m^{-3}$ for at least two consecutive days) were observed during these periods. The longest pollution episode lasted for 10 days (Fig. 2, EP6). The mean $PM_{2.5}$ concentrations during the seven severe pollution episodes were 96±16, 120±35, 98±11, 142±46, 154±46, 120±37, and 100±2 $\mu g \cdot m^{-3}$. During the severe pollution episodes, higher concentrations of SO_2 and NO_2 were observed. Furthermore, the low wind speed (WS) and high relative humidity (RH) promote the accumulation and secondary aerosol formation. The proportion of SNA was relatively high in $PM_{2.5}$, accounting for 49%, 69%, 49%, 66%, 63%, 50%, and 55% of the total $PM_{2.5}$ chemical composition during these episodes.

To prevent the spread of COVID-19, Hohhot implemented a Level I public health emergency response on January 25, 2020, which was subsequently adjusted to Level III on February 25. This study defined the strict control period as LD (January 25, 2020, to February 24, 2020) and the preceding month as pre-lockdown (pre-LD, December 25, 2019, to January 24, 2020). The mean concentrations of $PM_{2.5}$ during the pre-LD and LD were 89.4±52.3 and 58.3±49.7 $\mu g \cdot m^{-3}$, respectively. Compared to pre-LD, the mean concentrations of $PM_{2.5}$, NO_2, and CO during LD decreased by 31.0 $\mu g \cdot m^{-3}$ ($P<0.05$), 24.3 $\mu g \cdot m^{-3}$ ($P<0.001$), and 0.6 mg m^{-3} ($P<0.01$). The mean SO_2

https://doi.org/10.5194/egusphere-2023-1851
Preprint. Discussion started: 4 September 2023

concentration declined by 2.8 μg·m^{-3} (P>0.05). The decline in NO_2 and CO concentrations was related to the significant reduction in vehicular emissions. In addition to the reduction in AE, the significant decrease in $PM_{2.5}$ concentrations was also influenced by variations in MC.

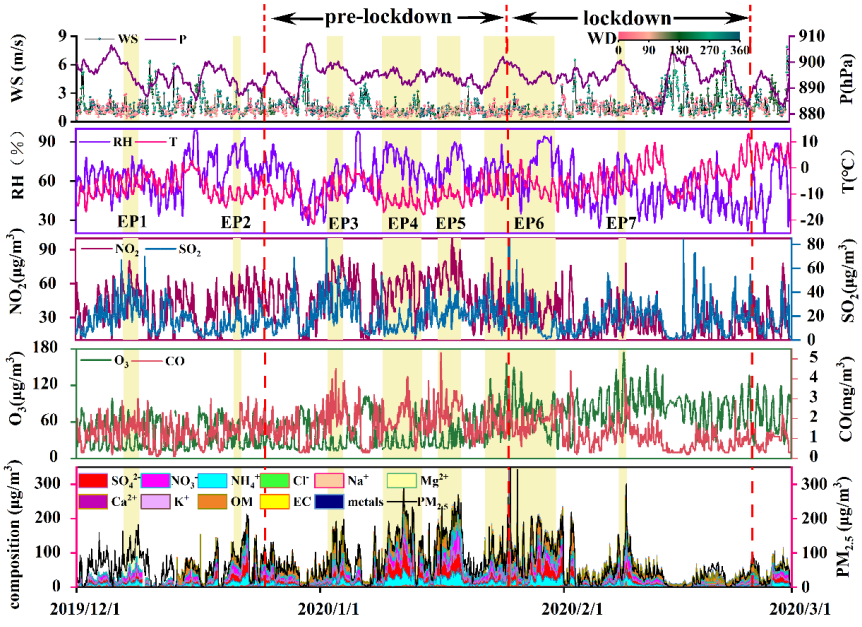

Figure 2. Variations in meteorological variables and atmospheric pollutants during the observation period (yellow background indicating severe pollution episodes)

3.2 Variations in $PM_{2.5}$ chemical constituents across different pollution levels

The concertation and percentage of $PM_{2.5}$ chemical composition are presented in Fig. 3 and Table S1. During the clean period ($PM_{2.5}$ <35 μg·m^{-3}), organic matter (OM) was the main composition (48%) of $PM_{2.5}$. From clean to severe pollution ($PM_{2.5}$ >150 μg·m^{-3}), the concentration of OM increased from 14 to 44 μg·m^{-3}; however, its proportion decreased from 48% to 26%. Compared to the clean period, the mean concentrations of SO_4^{2-}, NO_3^-, and NH_4^+ increased by 12, 9, and 10 times during severe pollution, respectively. Furthermore, the proportion of SNA increased from 32% to 61%, indicating that the rapid increase in secondary inorganic ions

https://doi.org/10.5194/egusphere-2023-1851
Preprint. Discussion started: 4 September 2023

significantly contributed to $PM_{2.5}$ aggravation. Especially for SO_4^{2-}, it was higher than that of NO_3^- in Hohhot, which is inconsistent with the results of megacities (Fu et al., 2020; Huang et al., 2019a; Yang et al., 2022b). Nitrate was the dominant component of SNA in Beijing since 2016, which could be attributed to the effective measure of SO_2 emissions (the precursor of SO_4^{2-}). Nitrate has become the predominant composition of $PM_{2.5}$ in Beijing (Fu et al., 2020). A similar result was also found in Zhongshan (Yang et al., 2022b). In Shanghai, NO_3^- was the most abundant species in winter, whereas SO_4^{2-} replaced NO_3^- as the dominant species in summer (Huang et al., 2019a). From clean to severe pollution, the concentrations of Cl^-, K^+, Na^+, Mg^{2+}, and metals in Hohhot increased by 4.2, 24.3, 0.03, 7.1, and 1.6 times, respectively, whereas the proportions of them decreased. The increase in Cl^-, K^+, and Mg^{2+} concentrations can be attributed to fireworks during the Spring Festival period (Li et al., 2022).

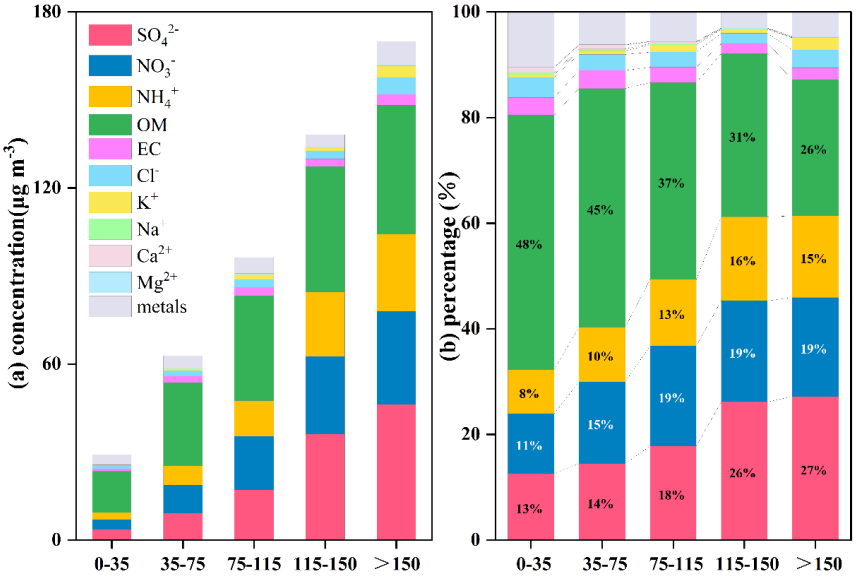

Figure 3. Variation in (a) concentration and (b) percentage of $PM_{2.5}$ chemical compositions at different pollution levels

https://doi.org/10.5194/egusphere-2023-1851
Preprint. Discussion started: 4 September 2023

3.3 Factors influencing $PM_{2.5}$ and its compositions

The correlations among the $PM_{2.5}$ chemical compositions, meteorological variables, and atmospheric pollutants are presented in Fig. S1. $PM_{2.5}$ negatively correlated with WS ($P<0.001$) and T ($P<0.01$). The lower WS and surface T (inversion) hinder $PM_{2.5}$ dispersion, thereby resulting in $PM_{2.5}$ accumulation. Furthermore, $PM_{2.5}$ positively correlated to SO_4^{2-}, NO_3^-, NH_4^+, SOR, NOR, and RH ($P<0.001$). High RH benefits the $PM_{2.5}$ hygroscopic growth (Liao et al., 2017) and secondary formation of SNA (Cheng et al., 2016), thereby exacerbating $PM_{2.5}$ pollution. However, when RH is higher than the threshold of 80%, the $PM_{2.5}$ concentration, SOR, and NOR decrease with increasing RH (Fig. 4). This may be related to the aggregation of suspended particles and sedimentation, thereby significantly reducing the $PM_{2.5}$ concentration (Cheng et al., 2015). In addition to RH, oxidation capacity ($Ox=O_3+NO_2$), and T are also considered to be vital factors influencing the formation of SO_4^{2-} and NO_3^-. During the observation period, SOR negatively correlated to T ($P<0.01$). The intensity of coal-fired heating was increased at lower T situations, resulting in increased SO_2 emissions in these periods. Especially, under low WS and high RH condition, the increase of SO_2 emissions leads to the rapid formation of SO_4^{2-}. SOR is not correlated with Ox ($P>0.05$), indicating that SO_4^{2-} was primarily formed through the aqueous-phase oxidation pathway. Typically, the photochemical oxidation rate of SO_2 is relatively slow (Zhang et al., 2015), whereas the aqueous-phase pathway plays a crutial role in SO_4^{2-} formation (Gao et al., 2016). Unlike SO_4^{2-}, Ox plays an essential role in NO_3^- formation. During the observation period, NOR positively correlated to Ox ($P<0.001$) and RH ($P<0.001$), indicating that photochemical and aqueous-phase oxidation both had a crucial role in NO_3^- formation in Hohhot. The homogeneous reaction between NO_2 and OH is the primary pathway for the daytime formation of HNO_3 (Finlayson-Pitts et al., 2003), and N_2O_5 hydrolysis is the primary pathway for the nighttime formation of HNO_3 (Pathak et al., 2011). Furthermore, HNO_3 can be converted to nitrate through reactions with alkaline species (Gard et al., 1998).

https://doi.org/10.5194/egusphere-2023-1851
Preprint. Discussion started: 4 September 2023

A higher OC/EC ratio was observed within the RH range of 20–40%, which may be attributed to the high Ox and T levels that promote SOC formation. Throughout the entire observation period, OC, EC, secondary organic carbon (SOC), and primary organic carbon (POC) showed positively correlated to RH ($P<0.001$) and Ox ($P<0.01$) and a significant negative correlation with T ($P<0.05$). This is primarily related to the increased intensity of coal-fired heating during low T, which often coincide with high RH. Furthermore, high RH promotes SOC formation (Huang et al., 2019b; Xu et al., 2017), whereas low T facilitates organic substances condensation (Galindo et al., 2019).

In conclusion, MC has a vital impact on $PM_{2.5}$ and its compositions. Therefore, this study utilized the RF model to evaluate the relative importance of time factors, meteorological variables, and gaseous pollutants in influencing $PM_{2.5}$ chemical composition (Fig. 5). The relative importance of SO_2, RH, and NO_2 was 28.4%, 19.7%, and 13.4% to $PM_{2.5}$, respectively, indicating that gaseous precursors and RH are the primary influencing factors for $PM_{2.5}$. This further confirms that under high RH conditions, the secondary formation of SO_4^{2-} and NO_3^- had a considerable contribution to $PM_{2.5}$ exacerbation (Han et al., 2016). Sulfate, NO_3^-, and NH_4^+ were the most sensitive to RH variation, and the relative importance values were 28.0%, 38.8%, and 33.1%, respectively. Nitrite exhibited sensitivity to O_X, whereas SO_4^{2-} and NH_4^+ demonstrated little sensitivity to O_X. It suggested that NO_3^- is significantly influenced by photochemical oxidation, whereas SO_4^{2-} is more affected by aqueous-phase oxidation. OC and SOC were sensitive to trends, SO_2, and NO_2, which can be attributed to periodic emissions variation.

https://doi.org/10.5194/egusphere-2023-1851
Preprint. Discussion started: 4 September 2023

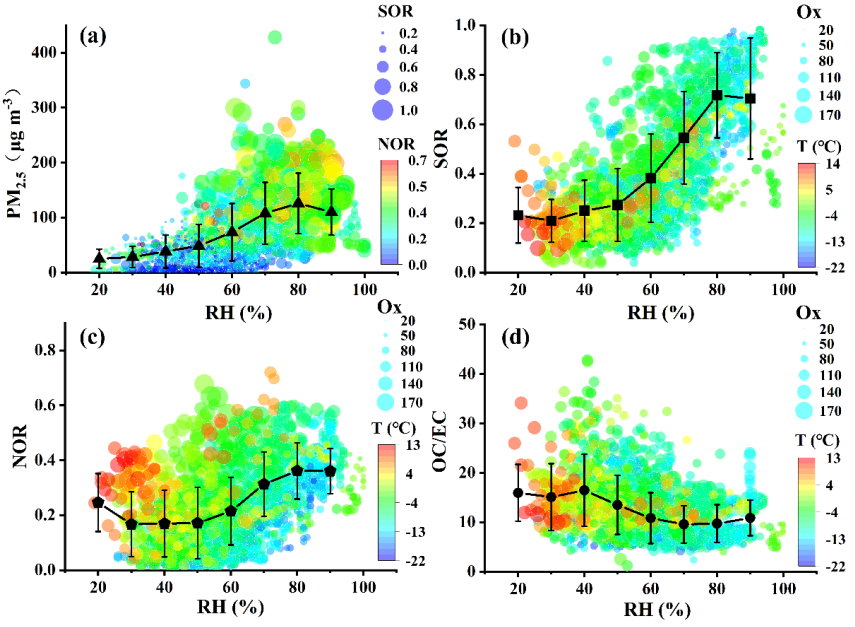

Figure 4. Corelations between RH and (a) $PM_{2.5}$, (b) SOR, (c) NOR, and (d) OC/EC

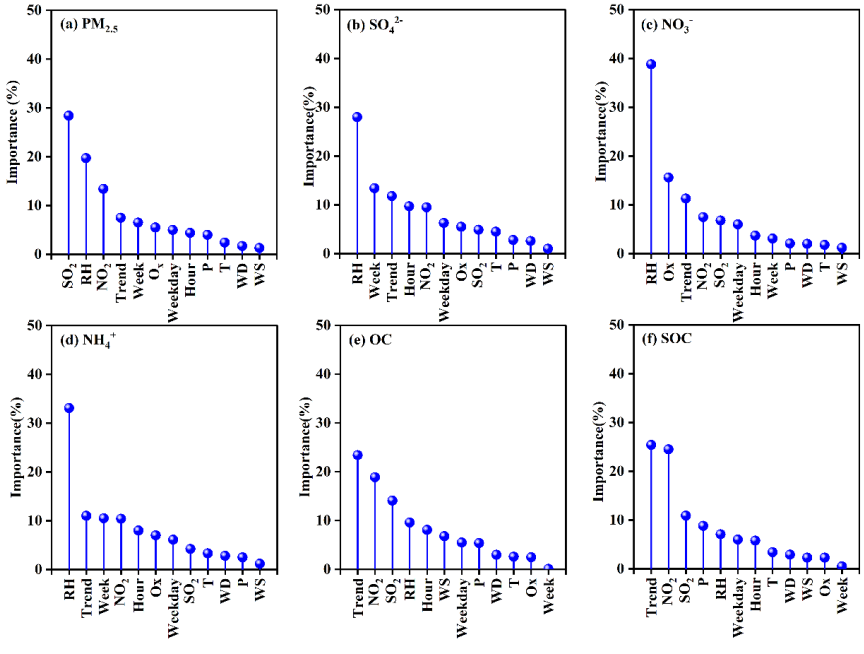

Figure 5. Relative importance of meteorological variables and atmospheric pollutants to (a) $PM_{2.5}$, (b) SO_4^{2-}, (c) NO_3^- , (d) NH_4^+, (e) OC, and (f) SOC

https://doi.org/10.5194/egusphere-2023-1851
Preprint. Discussion started: 4 September 2023

3.4 Response of $PM_{2.5}$ compositions to the variation of AE and MC

From clean to severe pollution, the contributions of AE and MC to $PM_{2.5}$ concentration increase by 1.1 and 4.5 times (Fig. 6), respectively, indicating that $PM_{2.5}$ concentration is more sensitive to variations in MC. During the clean period, MC contributed negatively to $PM_{2.5}$ concentrations, indicating that MC was conducive to pollutant dispersion. The contribution of MC increased with the increase of $PM_{2.5}$ concentration, with the highest contribution of 49% during severe pollution episodes. The MC contribution of SO_4^{2-}, NO_3^-, NH_4^+, OC, and SOC during severe pollution periods were 6.2, 3.9, 4.7, 3.6, and 3.1 times those of the clean period, respectively. The contribution of MC to SO_4^{2-}, NO_3^-, and NH_4^+ can reach 46%, 41%, and 35%, respectively. In conclusion, the rapid increase of SNA under adverse MC is the primary driver for $PM_{2.5}$ aggravation.

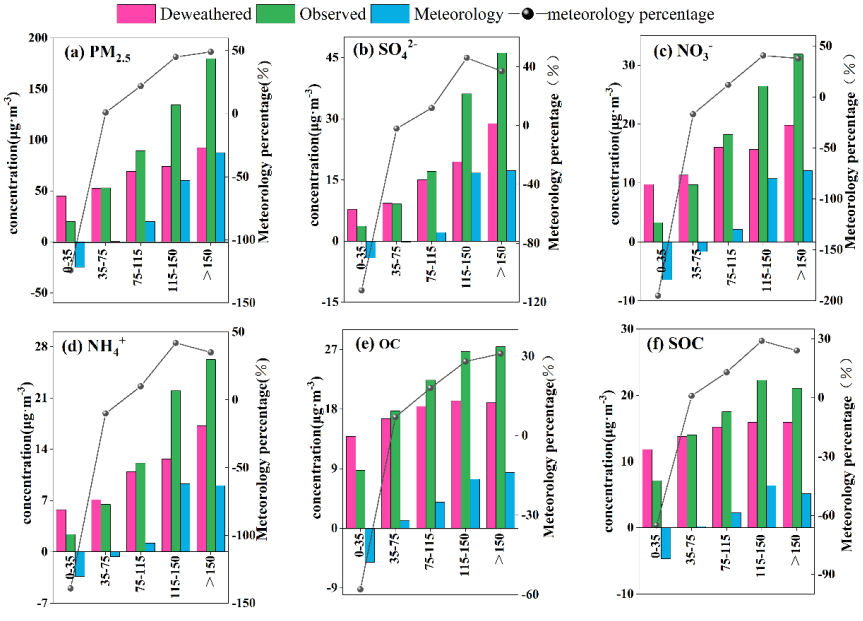

Figure 6. Contributions of AE and MC to (a) $PM_{2.5}$, (b) SO_4^{2-}, (c) NO_3^- , (d) NH_4^+, (e) OC, and (f) SOC at different pollution levels

The contributions of AE and MC to $PM_{2.5}$ major chemical compositions during the seven severe pollution episodes are presented in Fig. S2. The AE (MC)

https://doi.org/10.5194/egusphere-2023-1851
Preprint. Discussion started: 4 September 2023

contributed 64% (36%), 68% (32%), 71% (29%), 72% (28%), 78% (22%), and 83% (17%) to the $PM_{2.5}$, SO_4^{2-}, NO_3^-, NH_4^+, OC, and SOC concentrations, respectively. AE had a considerable contribution to all pollutants (>64%), whereas MC had a higher impact on $PM_{2.5}$, SO_4^{2-}, NO_3^-, and NH_4^+ (>28%).

Compared to the pre-LD, the temperatures (T) were higher during LD, in response to this variation the heating intensity had a considerable reduction, resulting in a 33% and 23% decrease in SO_2 and NO_X emissions, respectively (Fig. S3). Apart from heating enterprises, other key pollution sources have experienced a 22% decrease in SO_2 emissions, whereas NO_X emissions exhibited a relatively minor variation. Therefore, the substantial reduction of $PM_{2.5}$ and NO_2 concentrations during LD can be attributed to the combined effects of reduced heating intensity, lockdown control measures, decreased RH (from 65% to 54%), and increased WS (from 1.4 to 1.8 m/s). Compared to pre-LD, the concentration of O_3 exhibited a rapid increase during LD, with AE and MC contributing 19.8 and 22.7 $\mu g \cdot m^{-3}$, respectively. The swift increase in O_3 concentration during LD could be primarily attributed to the substantial reduction in NOx emissions, leading to a decreased titration of O_3 by NO (Wang et al., 2013). Specifically, AE contributed 16.2, 5.9, 3.2, 3.6, 2.0, and 2.1 $\mu g \cdot m^{-3}$ to the reductions in $PM_{2.5}$, SO_4^{2-}, NO_3^-, NH_4^+, OC, and SOC, which accounted for 52%, 81%, 48%, 68%, 59%, and 288% of the total variation, respectively. MC contributed 14.8, 1.4, 3.5, 1.7, 1.4, and -1.4 $\mu g \cdot m^{-3}$ to the variations in $PM_{2.5}$, SO_4^{2-}, NO_3^-, NH_4^+, OC, and SOC, which accounted for 48%, 19%, 52%, 32%, 41%, and -188% of the total variations, respectively. The lockdown measures had a significant reduction effect on SO_2 and NO_2 concentrations, with 138% (-38%) and 82% (18%) attributed to AE (MC), respectively.

https://doi.org/10.5194/egusphere-2023-1851
Preprint. Discussion started: 4 September 2023

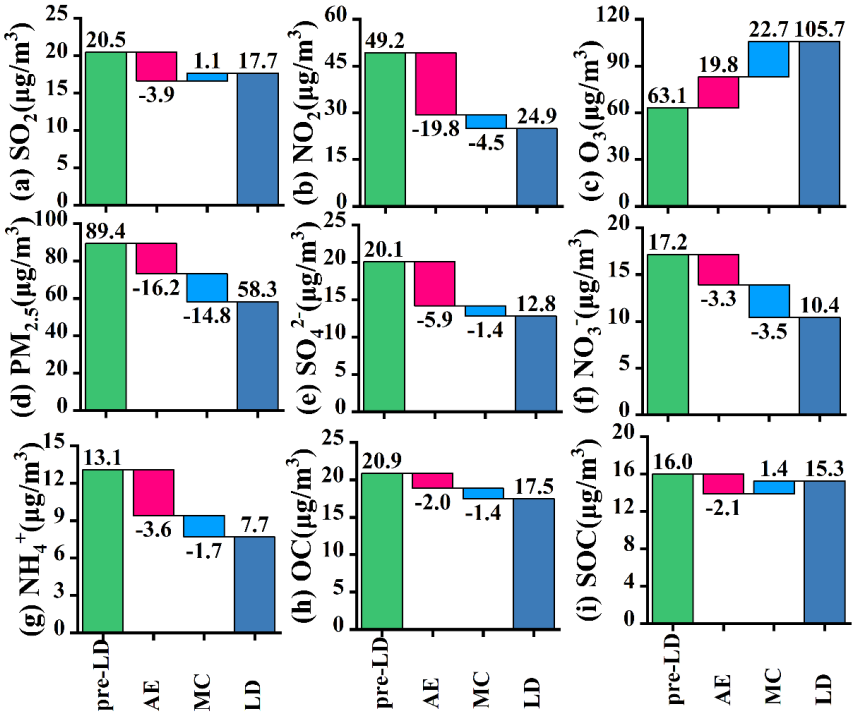

265 Figure 7. Contributions of AE and MC to variations in (a) SO_2, (b) NO_2, (c) O_3, (d) $PM_{2.5}$, (e) SO_4^{2-}, (f) NO_3^- , (g) NH_4^+, (h) OC, and (i) SOC during the pre-LD and LD periods.

4. Conclusion

To reveal the causes of pollution episodes and the relationship among 270 atmospheric pollutants, AE, and MC, online observations of $PM_{2.5}$ and its chemical compositions were conducted in Hohhot during the winter season. SNA was the predominant composition of $PM_{2.5}$ in Hohhot, particularly during severe pollution episodes. The concentration and proportion of SNA increased rapidly from clean to severe pollution episodes. The formation of SO_4^{2-} in winter was primarily attributed to 275 aqueous-phase oxidation, whereas both aqueous-phase and photochemical oxidation played vital roles in NO_3^- formation. The results from the RF model indicated that

https://doi.org/10.5194/egusphere-2023-1851
Preprint. Discussion started: 4 September 2023

gaseous pollutants (SO_2 and NO_2) and MC (RH) had significant impacts on $PM_{2.5}$. SNA was the most sensitive to RH. From clean to severe pollution, MC had a considerable contribution to the SNA concentrations, suggesting that the rapid generation of SNA was the driving factor of $PM_{2.5}$ aggravation in Hohhot. The lockdown measures contributed to the reduction of most of the pollutants, whereas variations in MC contributed significantly to the decrease of $PM_{2.5}$ and NO_3^- levels during the LD. Therefore, when assessing the effectiveness of pollution control policies in the future, it is essential to fully consider the contribution of MC to pollutants.

Acknowledgments

This work was supported by the National Natural Science Foundation of China (42167015) and Science and Technology Project of Inner Mongolia Autonomous Region (2022YFHH0126).

References

An Z, Huang R-J, Zhang R, et al., 2019. Severe haze in northern China: A synergy of anthropogenic emissions and atmospheric processes. Proceedings of the National Academy of Sciences 116, 8657-8666.

Chen X, Li X, Liang J, et al., 2023. Causes of the unexpected slowness in reducing winter $PM_{2.5}$ for 2014–2018 in Henan Province. Environmental Pollution 319, 120928.

Cheng Y, He K-b, Du Z-y, et al., 2015. Humidity plays an important role in the $PM_{2.5}$ pollution in Beijing. Environmental Pollution 197, 68-75.

Cheng Y, Zheng G, Wei C, et al., 2016. Reactive nitrogen chemistry in aerosol water as a source of sulfate during haze events in China. Science Advances 2, e1601530.

Dominici F, McDermott A, Zeger SL, et al., 2002. On the Use of Generalized Additive Models in Time-Series Studies of Air Pollution and Health. American Journal of Epidemiology 156, 193-203.

Feng S, Jiang F, Wang H, et al., 2020. NOx Emission Changes Over China During the COVID-19 Epidemic Inferred From Surface NO_2 Observations. Geophysical Research Letters 47, e2020GL090080.

https://doi.org/10.5194/egusphere-2023-1851
Preprint. Discussion started: 4 September 2023

Finlayson-Pitts BJ, Wingen LM, Sumner AL, et al., 2003. The heterogeneous hydrolysis of NO_2 in laboratory systems and in outdoor and indoor atmospheres: An integrated mechanism. Physical Chemistry Chemical Physics 5, 223-242.

Fu X, Wang T, Gao J, et al., 2020. Persistent Heavy Winter Nitrate Pollution Driven by Increased Photochemical Oxidants in Northern China. Environmental Science & Technology 54, 3881-3889.

Fuzzi S, Baltensperger U, Carslaw K, et al., 2015. Particulate matter, air quality and climate: lessons learned and future needs. Atmos. Chem. Phys. 15, 8217-8299.

Galindo N, Yubero E, Clemente A, et al., 2019. Insights into the origin and evolution of carbonaceous aerosols in a mediterranean urban environment. Chemosphere 235, 636-642.

Gao M, Carmichael GR, Wang Y, et al., 2016. Improving simulations of sulfate aerosols during winter haze over Northern China: the impacts of heterogeneous oxidation by NO_2. Frontiers of Environmental Science & Engineering 10, 16.

Gard EE, Kleeman MJ, Gross DS, et al., 1998. Direct Observation of Heterogeneous Chemistry in the Atmosphere. Science 279, 1184-1187.

Grange SK, Carslaw DC, Lewis AC, et al., 2018. Random forest meteorological normalisation models for Swiss PM_{10} trend analysis. Atmos. Chem. Phys. 18, 6223-6239.

Guo Y, Li K, Zhao B, et al., 2022. Evaluating the real changes of air quality due to clean air actions using a machine learning technique: Results from 12 Chinese mega-cities during 2013–2020. Chemosphere 300, 134608.

Han B, Zhang R, Yang W, et al., 2016. Heavy haze episodes in Beijing during January 2013: Inorganic ion chemistry and source analysis using highly time-resolved measurements from an urban site. Science of The Total Environment 544, 319-329.

He J, Gong S, Yu Y, et al., 2017. Air pollution characteristics and their relation to meteorological conditions during 2014–2015 in major Chinese cities. Environmental Pollution 223, 484-496.

Huang L, An J, Koo B, et al., 2019a. Sulfate formation during heavy winter haze events and the potential contribution from heterogeneous $SO_2 + NO_2$ reactions in the Yangtze River Delta region, China. Atmos. Chem. Phys. 19, 14311-14328.

https://doi.org/10.5194/egusphere-2023-1851
Preprint. Discussion started: 4 September 2023

Huang RJ, Wang Y, Cao J, et al., 2019b. Primary emissions versus secondary formation of fine particulate matter in the most polluted city (Shijiazhuang) in North China. Atmos. Chem. Phys. 19, 2283-2298.

Huang X, Ding A, Gao J, et al., 2021. Enhanced secondary pollution offset reduction of primary emissions during COVID-19 lockdown in China. National Science Review 8, nwaa137.

Li Z, Yu S, Li M, et al., 2022. Non-stop industries were the main source of air pollution during the 2020 coronavirus lockdown in the North China Plain. Environmental Chemistry Letters 20, 59-69.

Liao T, Wang S, Ai J, et al., 2017. Heavy pollution episodes, transport pathways and potential sources of $PM_{2.5}$ during the winter of 2013 in Chengdu (China). Science of The Total Environment 584-585, 1056-1065.

Lv Y, Tian H, Luo L, et al., 2023. Understanding and revealing the intrinsic impacts of the COVID-19 lockdown on air quality and public health in North China using machine learning. Science of The Total Environment 857, 159339.

Pathak RK, Wang T, Wu WS, 2011. Nighttime enhancement of $PM_{2.5}$ nitrate in ammonia-poor atmospheric conditions in Beijing and Shanghai: Plausible contributions of heterogeneous hydrolysis of N_2O_5 and HNO_3 partitioning. Atmospheric Environment 45, 1183-1191.

Vu TV, Shi Z, Cheng J, et al., 2019. Assessing the impact of clean air action on air quality trends in Beijing using a machine learning technique. Atmos. Chem. Phys. 19, 11303-11314.

Wang J, Hu Z, Chen Y, et al., 2013. Contamination characteristics and possible sources of PM_{10} and $PM_{2.5}$ in different functional areas of Shanghai, China. Atmospheric Environment 68, 221-229.

Wang P, Chen K, Zhu S, et al., 2020. Severe air pollution events not avoided by reduced anthropogenic activities during COVID-19 outbreak. Resources, Conservation and Recycling 158, 104814.

WHO. World Health Organization, Regional Office for Europe. Air Quality Guidelines: Global Update 2005: Particulate Matter, Ozone, Nitrogen Dioxide, and Sulfur Dioxide, 2021.

Xu W, Han T, Du W, et al., 2017. Effects of Aqueous-Phase and Photochemical Processing on Secondary Organic Aerosol Formation and Evolution in Beijing, China. Environmental Science & Technology 51, 762-770.

Yang F, Tan J, Zhao Q, et al., 2011. Characteristics of $PM_{2.5}$ speciation in representative megacities and across China. Atmos. Chem. Phys. 11, 5207-5219.

https://doi.org/10.5194/egusphere-2023-1851
Preprint. Discussion started: 4 September 2023

Yang K, Wu C, Luo Y, 2022a. The impact of COVID-19 on urban $PM_{2.5}$ -taking Hubei Province as an example. Environmental Pollution 294, 118633-.

Yang Y, Zhang Z, Yang Y, et al., 2022b. Impact of high $PM_{2.5}$ nitrate on visibility in a medium size city of Pearl River Delta. Atmospheric Pollution Research 13, 101592.

Zhang B, Zhang Y, Zhang K, et al., 2023. Machine learning assesses drivers of $PM_{2.5}$ air pollution trend in the Tibetan Plateau from 2015 to 2022. Science of The Total Environment 878, 163189.

Zhang Q, He K, Huo H, 2012. Cleaning China's air. Nature 484, 161-162.

Zhang Q, Zheng Y, 2019. Drivers of improved $PM_{2.5}$ air quality in China from 2013 to 2017. Proceedings of the National Academy of Sciences 116, 24463-24469.

Zhang R, Wang G, Guo S, et al., 2015. Formation of Urban Fine Particulate Matter. Chemical Reviews 115, 3803-3855.